34th IAHR World Congress − Balance and Uncertainty
33rd Hydrology & Water Resources Symposium
10th Hydraulics Conference

26 June − 1 July 2011, Brisbane, Australia

Dam Breaks Of Viscoplastic Material On An Inclined Plane

S. Cochard[1], and C. Ancey[2]

[1]Faculty of Engineering and Information Technology
The University of Sydney
Sydney NSW 2006
AUSTRALIA

[2]Environmental Hydraulic Laboratory
Ecole Polytechnique Fédérale de Lausanne
1015 Lausanne
SWITZERLAND
E-mail: steve.cochard@sydney.edu.au

Abstract: *We report experimental results related to the dam-break problem for viscoplastic fluids. Using image processing techniques, we were able to accurately reconstruct the free-surface evolution of fixed volumes of fluid suddenly released on an inclined plane. Carbopol Ultrez 10 was used as a viscoplastic material. Varying the Carbopol concentration allowed us to change the yield stress and bulk viscosity. We investigated the behaviour of a 43-kg mass released on a plane, whose inclination ranged from 0◦ to 18◦. For each run, we observed that the behaviour was nearly the same: at short times, the mass accelerated vigorously on gate opening and very quickly reached a nearly constant velocity. At time t = 1 s, independently of plane inclination and yield stress, the mass reached a near-equilibrium regime, where the front position varied as a power function of time over several decades. We did not observe any run-out phase, during which the mass would have gradually come to a halt.*

Keywords: *Dam break problem, viscoplastic fluid, flow visualization.*

1. INTRODUCTION

The shallow-water equations were originally derived by Saint Venant (1871) to compute flood propagation along rivers. They were gradually adapted to strongly time-dependent flows such as waves induced by a dam break (Ritter, 1892). A growing number of models based on the shallow-water equations are currently being used to describe natural flows such as flash floods (Hogg and Pritchard, 2004), floods with sediment transport (Pritchard, 2005), snow avalanches (Bartelt et al, 1999), debris flows (Iverson, 1997; Huang & García, 1997), lava flows (Griffiths, 2000), subaqueous avalanches (Parker et al, 1986), and so on. In the derivation of these models, a number of assumptions are used, the most important of which are: the long-wave approximation (no significant curvature of the free surface), hydrostatic pressure, blunt velocity profile, and no change in the bulk composition and rheology. Furthermore, in these models, the bottom shear stress is computed using either empirical expressions (e.g., Chézy friction) or non-Newtonian constitutive equations, with the difficult question of parameter estimation remaining. Given the number of approximations and assumptions needed to obtain these models, one can legitimately be suspicious of their reliability and performance. In this paper, we report experimental results of dam-break flows involving fixed volumes of viscoplastic materials.

2. EXPERIMENTAL SETUP

To investigate avalanching masses of fluid, we built an experimental setup made up of a high-rigidity metal frame supporting a reservoir, a 6-mm-thick aluminum plate, and a horizontal run-out zone. This full facility was 5.5 m long, 1.8 m wide, and 3.5 m high. The plate could be inclined from 0° to 45. Its position was accurately controlled using a digital inclinometer with a resolution of 0.1°.
The reservoir was positioned at the top of the inclined plane behind the lock gate. The reservoir was 51 cm long and 30 cm wide. The maximum capacity of the reservoir was 120 kg. The dam wall was composed of a 1.6 x 0.8 m^2 ultra-light carbon plate (which was 4 cm thick). Two pneumatic jacks opened the sluice gate to the desired aperture within 0.8 s. An ultra-light lock gate was needed to reduce gate inertia and plane vibration. The two jacks were quickly raised by injecting pressurized air

at 7 MPa. Two electromagnetic sensors were located at the tip of each jack to control its position and start the clock.

To measure the free-surface shape, we developed a novel imaging system, which consisted of a high-speed digital camera (a Basler A202k) coupled to a synchronized micro-mirror projector (a modified z-Snapper provided by ViALUX, Chemnitz, Germany). The camera recorded how regular patterns projected onto the surface were deformed when the free surface moved (see Figure 1). We developed algorithms to process the image data, determine the spreading rate, and reconstruct whole-field three-dimensional shapes of the free surface. The free surface was reconstructed with an accuracy of 1 mm over a surface of 1.4 x 1.4 m^2 at a rate of 45 Hz (further details of the experimental procedure are provided by Cochard & Ancey (2008)).
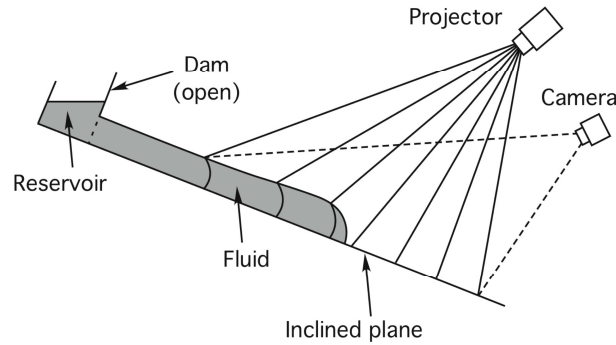

Figure 1 The Sketch of the experimental setup and the measurement system

2.1. Viscoplastic fluid

We used Carbopol Ultrez 10, a viscoplastic stable polymeric gel. This is a carbomer polymeric gel produced by Noveon. Hereafter and unless specified otherwise, Carbopol refers to Carbopol Ultrez 10. Carbopol was used at four different concentrations. Table 1 summarizes the concentration of the different components used. To describe the rheological behavior of Carbopol, we used the Herschel-Bulkley model, whose expression for a simple-shear flow is

$$\tau = \tau_c + K\dot{\gamma}^n \qquad (1)$$

with τ_c the yield stress, K the consistency, and n an index. We determined the value of these parameters from rheometrical experiments. A full description of the preparation procedure is described in Cochard (2007).

Table 1 Rheological characteristics and composition of the Carbopol samples used (for a 60-kg mass).

Concentration C	0.25%	0.30%	0.35%	0.40%
Carbopol Ultrez 10 [g]	150.00±0.05	180.00±0.05	210.00±0.05	240.00±0.05
NaOH [g]	62.20±0.05	74.64±0.05	87.09±0.05	99.53±0.05
H$_2$O [kg]	79.79±0.04	59.07±0.04	58.92±0.04	58.77±0.04
Solution [kg]	60.00±0.04	60.00±0.04	60.00±0.04	60.00±0.04
τ_c [Pa]	78±1	89±1	102±1	109±1
K [Pa s^{-1}]	32.1±2.3	47.7±1.7	58.9±1.7	75.8±1.9
n [-]	0.388±0.023	0.415±0.021	0.505±0.027	0.579±0.033

3. EXPERIMENTAL RESULTS

The spreading of the avalanching mass depended on the fluid rheological parameters (τ_c, K, and n), the plane inclination (α), the reservoir dimensions, and the mass (m). To evaluate the influence of the rheological parameters and plane inclination on propagation, we kept the mass (43 kg) and the

reservoir dimensions constant while the concentration and the plane inclination were varied. Sixteen tests were carried out with a 43 kg mass of Carbopol at concentrations C = 0.25, 0.30, 0.35, and 0.40% for plane inclination α of 0, 6, 12, and 18°.

3.1. Flow regimes observed

We first describe the typical behaviour of an avalanching mass. Figure 2 (a) through (e) are snapshots of a typical experiment (here obtained with a 12° slope and concentration set to C = 0.30%). The time variations in the flow-depth profile and front position are reported in Figure 3 while the contact lines are shown in Figure 4. We observed the following behaviour:

(a) At time t = 0.19 s, the dam gate was being raised. At that time, the effective aperture was 8 cm. The gel was pushed out of the reservoir as a result of hydrostatic pressure. The free surface was nose-shaped. The surge motion was mainly in the x-direction.

(b) At time t = 0.48 s, the dam gate was still being lifted. The aperture was 17 cm, which was still lower than the fluid height in the reservoir (which was about 33 cm). The free surface exhibited strong curvature. Since most of the mass was sheared, the mass behaved as a liquid with no visible unsheared zone. The velocity in the x-direction was about 4 times higher than that in the y-direction.

(c) At time t = 0.80 s, the gate was fully open. The fluid was still in an inertial regime, i.e. the dynamics was governed by the balance between inertia and pressure-gradient terms. Note that following the gate opening, part of the fluid immediately moved downstream in the form of a forward wave, while a wave propagating upstream separated moving fluid from static fluid upslope. The latter reached the rear end at t = 0.6 s.

(d) At time t = 1.60 s, the gel had slowed down drastically (see Figure 3). Time variations in the velocity became increasingly smaller, indicating that the gel reached a near-equilibrium regime where the dominant forces were the viscous forces and gravity acceleration. The flow-depth gradient in the streamwise direction was close to zero except for the tip region.

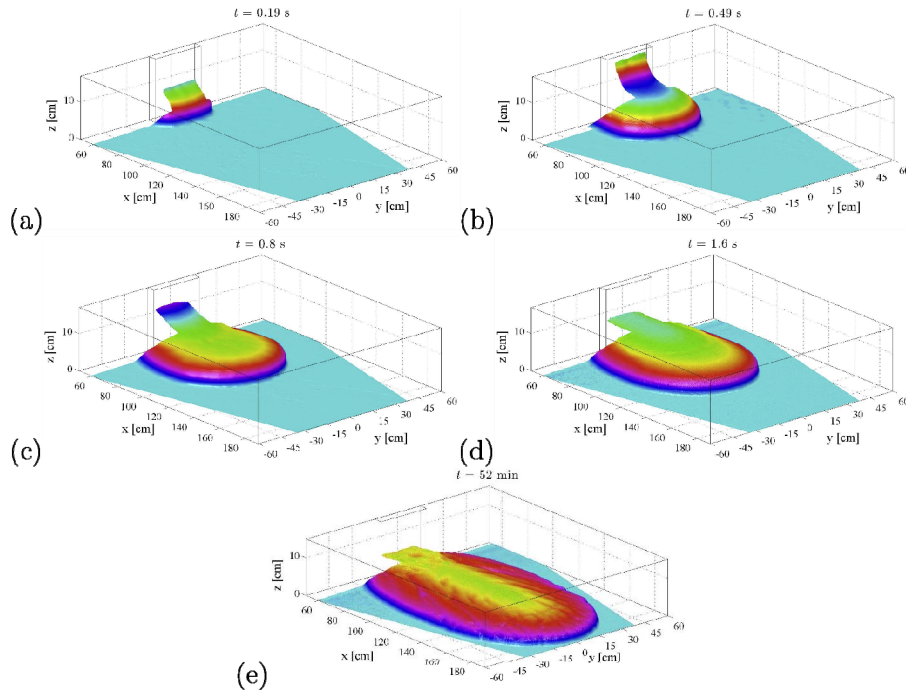(e) At time t = 52 min, the gel was still moving at 12 cm/h and channelization could be observed.

Figure 2 Three-dimensional view of a 43-kg avalanching mass of Carbopol (C = 0.30%) and α = 12° at time: (a) t = 0.19 s. (b) t = 0.48 s. (c) time t = 0.80s. (d) t = 1.60 s. (e) t = 52 min.

In brief, we observed two regimes: at the very beginning ($t \leq 1$ s), the flow was in an inertial regime; the front velocity was nearly constant. Then, quite abruptly, a pseudo-equilibrium regime occurred, for which the front velocity decayed as a power-law function of time.

The inertia regime depends on the mass of fluids as well as the initial height. The same mass of fluid, in a different reservoir, leading to another initial height would have resulted in a different behavior of the inertia regime.
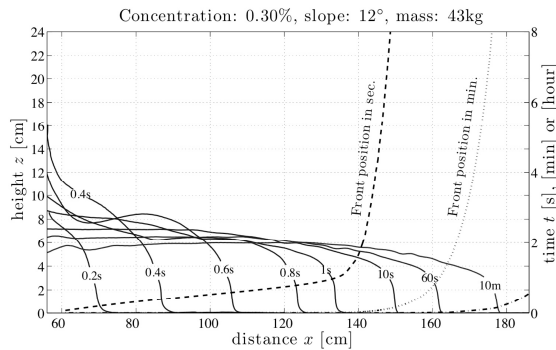

Figure 3 Surge profile and front position for a 43-kg avalanching mass of Carbopol ($C = 0.30\%$) down a 12° inclined plane.
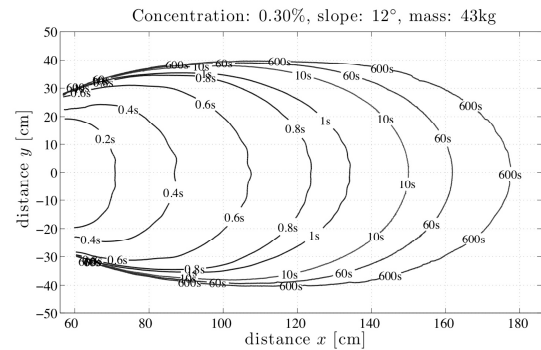
Figure 4 Contact line for a 43-kg avalanching mass of Carbopol ($C = 0.30\%$) down a 12° inclined plane.

3.2. Front position, contact line, and flow-depth profile

Figure 5 and Figure 6 summarize the measurements taken for each run. In a condensed form, we plot the flow-depth profile (measured at the centerline), the contact line, and the evolution of the front position. Each column in Figure 5 and Figure 6 is related to a fixed inclination (0, 6, 12, and 18°) while the rows present results corresponding to the same Carbopol concentration (0.25, 0.30, 0.35 and 0.40%). For each plot, the flow-depth profiles taken at time $t = 0.4, 0.8, 2, 20, 200, 2 \cdot 10^3$, and $2 \cdot 10^4$ s are reported in the upper half part; the left axis gives elevation z. The contact lines measured at the same time as the flow-depth profiles are plotted in the lower half part of the plot.

The front position x_f is plotted as a function of time in a log-linear diagram; time t is reported on the right axis. Note that $x = 0$ corresponds to the rear end of the reservoir, while the 4-cm thick gate is located at $x = 51\text{-}55$ cm.

To guarantee an accurate measurement of the surge free surface, the acquisition setup was positioned to record from $x = 55$ cm (the position of the dam-gate) to $x = 190$ cm. The acquisition was stopped once the front position x_f had reached 190 cm or after 8 hours.

As expected, we observed that gels with the lowest Carbopol concentrations flowed faster and farther. Similarly, the steeper the inclination was, the faster the flows. Comparing the plots in Figure 5 and 6 leads to further interesting observations:

- The typical duration T_i of the inertia-dominated regime was on the order of 1 s. Taking a closer look at our data reveals a slight dependence of T_i on plane inclination. Strikingly enough, T_i seems to be independent of Carbopol concentration C, although the front position and velocity were influenced by C. A typical example is provided in Figure 7, where we report the front position as a function of time for $\alpha = 12°$ and different C values. For all concentrations, T_i was about 1 s. The distance at which the transition from an inertial to a near equilibrium regimes was observed depended on solid concentration: it increased from 120 cm to 145 cm when the concentration was increased from 0.25 to 0.4%.

- During the inertial phase, the front velocity was nearly constant (e.g., see Figure 3). This contrasts somehow with what we know of inertial flows. For inviscid fluids instantaneously released on a dry horizontal plane, dam-break theory predicts that the front velocity u_f does not vary with time, but solely with the initial flow depth h_0: $u_f = \sqrt{2gh_0}$ (Ritter's solution); for sloping beds, the front is continuously accelerating Ancey (2008). If we take the example of Figure 3, the front velocity was about 70 cm/s, whereas an estimate of the front velocity for the Ritter solution is $u_f = 2.4$ m/s, i.e. a factor of 3.5 higher than the velocity observed. This clearly shows that even in the inertia-dominated regime, viscous dissipation played a non-negligible role.
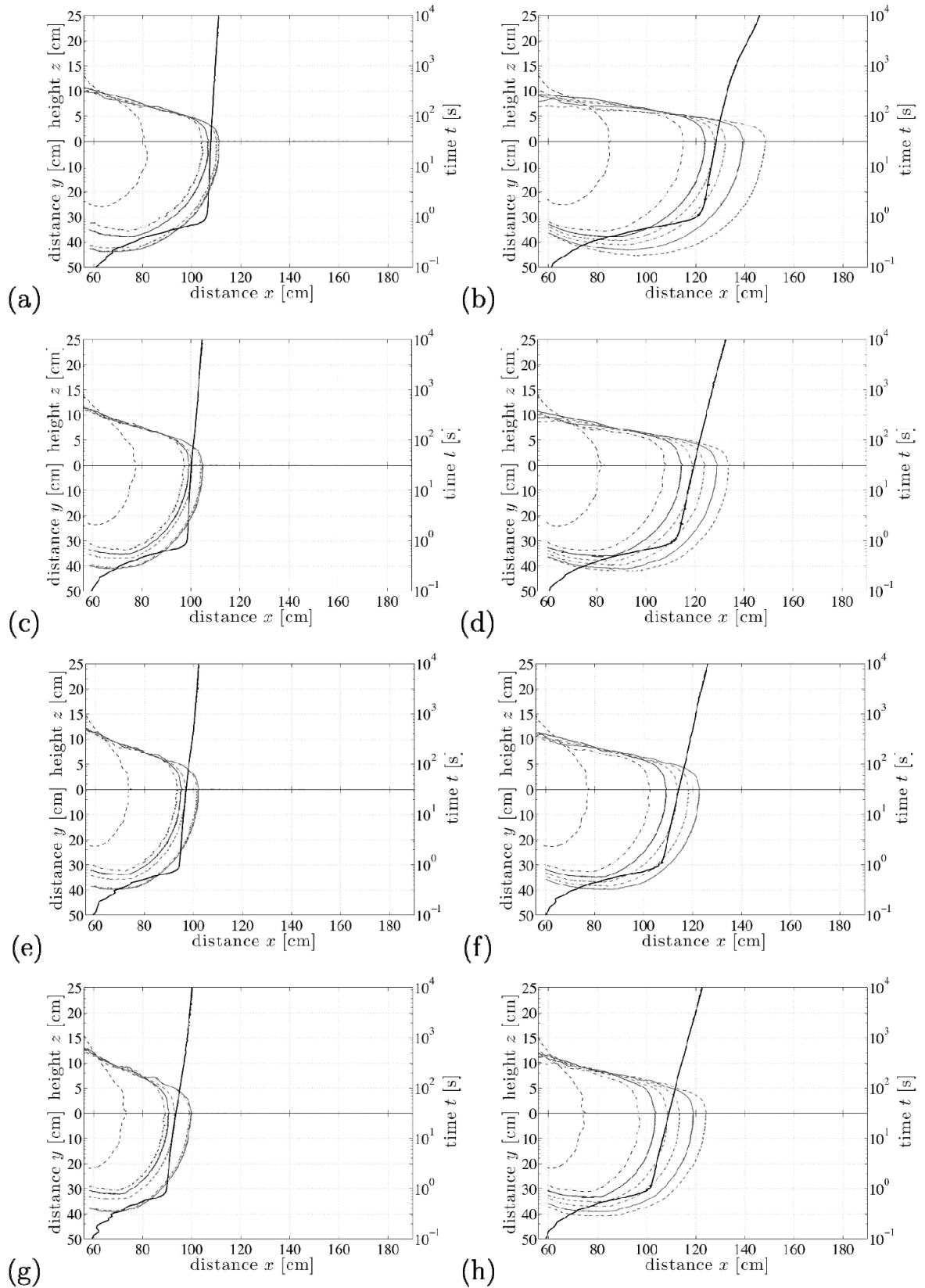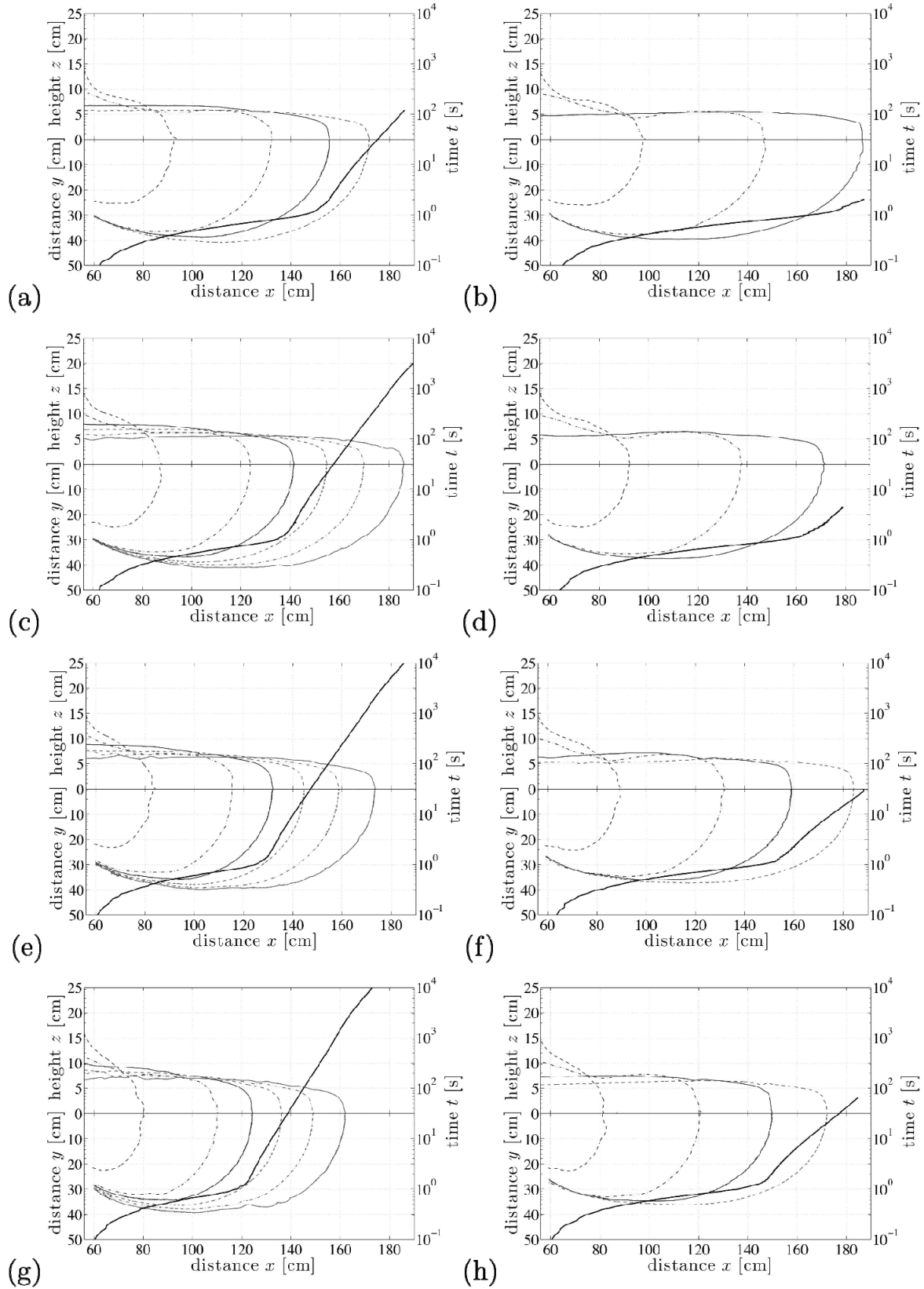
Figure 5 Flow-depth profiles and contact line at t = 0.4 (dashed line), 0.8 (dashed– dotted line), 2 (solid line), 20 (dashed line), 200 (dashed-dotted line), 2000 (solid line) and 20,000 s (dashed line). Time variation in the front position. Experimental conditions: (a) $\alpha = 0°$ and $C = 0.25\%$. (b) $\alpha = 6°$ and $C = 0.25\%$. (c) $\alpha = 0°$ and $C = 0.30\%$. (d) $\alpha = 6°$ and $C = 0.30\%$. (e) $\alpha = 0°$ and $C = 0.35\%$. (f) $\alpha = 6°$ and $C = 0.35\%$. (g) $\alpha = 0°$ and $C = 0.40\%$. (h) $\alpha = 6°$ and $C = 0.40\%$.

Figure 6 Flow-depth profiles and contact line at t = 0.4 (dashed line), 0.8 (dashed– dotted line), 2 (solid line), 20 (dashed line), 200 (dashed-dotted line), 2000 (solid line) and 20,000 s (dashed line). Time variation in the front position. Experimental conditions: (a) α = 12° and C = 0.25%. (b) α = 18° and C = 0.25%. (c) α = 12° and C = 0.30%. (d) α = 18° and C = 0.30%. (e) α = 12° and C = 0.35%. (f) α = 18° and C = 0.35%. (g) α = 12° and C = 0.40%. (h) α = 18° and C = 0.40%.
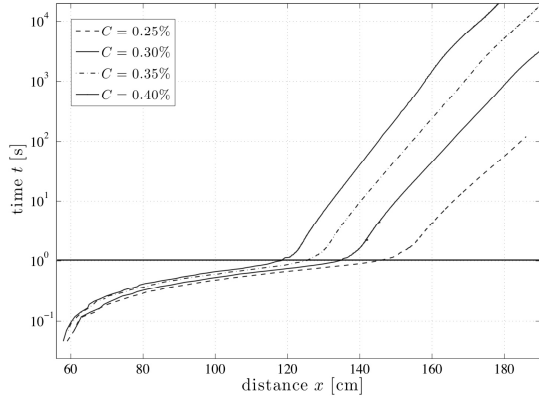
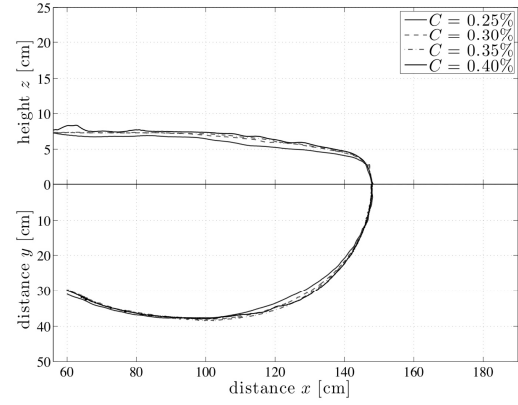**Figure 7 Front position x_f in function of the time t for a slope angle α = 12°.**

Figure 8 Surge profile and contact line for a front position x_f = 138 cm and α = 12°.

- The shape of the free surface depended a great deal on slope, but weakly on Carbopol concentration. Figure 8 reports the flow-depth profile together with the contact line for 4 different concentrations in Carbopol. All measurements were taken for a 12° inclination and when the front reached the position x_f = 38 cm. Note that all profiles were quite similar. Interestingly enough, we can also point out that the flows were in a near-equilibrium regime except for the flow at C = 0.25% (which was still in an inertia-dominated regime). The maximum height difference was on the order of 6 mm, while the maximum difference in the lateral spread was lower than 2 cm. As shown in Figure 9 where we plot the flow-depth profile and contact line for α = 6° and 18° (other parameters being the same), slope has great influence on the free-surface shape.
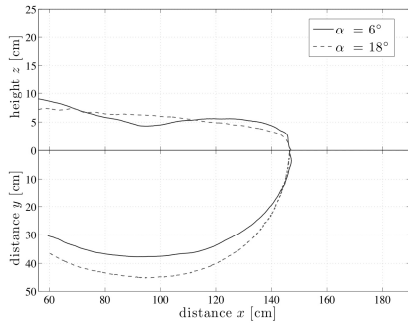

Figure 9 Surge profile and contact line for α = 6° and 12°.
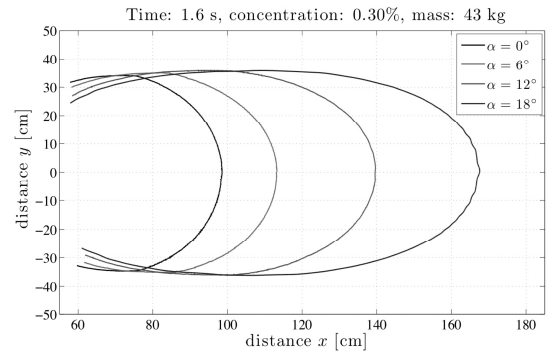

Figure 10 Contact line at time t =1.6 s for Carbopol at a concentration of 0.30% down inclined planes.

- Lateral spreading mostly occurred during the inertial phase, as seen on each plot of Figure 5 and Figure 6. Plane inclination had little influence on lateral spreading, as illustrated in Figure 10 where the contact lines are reported for different slopes α = 0, 6, 12, and 18°; the Carbopol concentration was the same (C = 0.3%) and the contact lines were recorded at the same time t = 1.6 s.
- We did not observe any avalanching mass coming to a halt, even at shallow slope and with large-yield-stress fluids. This supports the theoretical analysis carried out by Matson & Hogg (2006) and Balmforth et al (2007) for the dam-break problem on horizontal planes.

4. CONCLUSION

To gain insight into the complex behavior of time-dependent, free-surface flows of viscoplastic

materials, we built up an experimental setup, which makes it possible to carefully investigate the dam-break problem on horizontal and sloping beds in the laboratory. To track the free-surface evolution, a novel imaging system, made up of a high-speed digital camera coupled to a synchronized micro-mirror projector, was designed and used. The precision of the measurement system is on the order of 1 mm on a 1.4 × 1.4 m^2 surface at a rate of 45 Hz.

This paper focuses on the behavior of a large mass of Carbopol suddenly released on a sloping plane. As a first approximation, Carbopol behaves like a Herschel-Bulkley fluid. Sixteen tests were carried out with a 43 kg mass of Carbopol at 4 different concentrations, C = 0.25, 0.30, 0.35, and 0.40%. The plane inclination ranges from 0 to 18°. The mass and the reservoir dimensions were kept constant. By comparing all runs, it can be observed that the behavior was nearly the same for each run: at the very beginning, the mass accelerated vigorously on gate opening. Although it had some similarities with fully inertial phases observed for inviscid and Newtonian fluids, substantial differences are observed; in particular, the front velocity was constant and much lower than the front velocity given by the Ritter solution to the dam-break problem.

5. ACKNOWLEDGMENTS

6. REFERENCES

Ancey, C., Rentschler, M., Iverson, R and Denlinger, R.D (2008), *An exact solution for ideal dam-break floods on steep slopes,* Water Resour. Res. 44

Balmforth, N., Craster, R., Rust, A. and R. Sassi, R. (2007), *Viscoplastic flow over an inclined surface*, J. Non-Newtonian Fluid Mech. 142 219–243.

Bartelt, P., Salm, B. and Gruber, U. (1999), *Calculating dense- snow avalanche run out using a Voellmy-fluid model with active/passive longitudinal straining,* J. Glaciol. 45:242–254

Cochard, S. and Ancey, C. (2008), *Tracking the free surface of time-dependent flows: Image processing for the dam-break problem*, Exp. in. Fluids 44 (2008)59–71.

Cochard, S. (2007*), Measurements of time-dependent free-surface viscoplastic flows down steep slopes*, Ph.D. thesis, Ecole Polytechnique Fédérale de Lausanne, Lausanne, Switzerland.

Griffiths, R. (2000), *The dynamics of lava flows*, Ann. Rev. Fluid Mech. 32:477–518

Hogg, A. and Pritchard, D. (2004), *The effects of hydraulic resistance on dam-break and other shallow inertial flows,* J. Fluid Mech. 501:179–212

Huang, X., García, M. (1997), *A perturbation solution for Bingham-plastic mudflows,* J. Hydr. Eng. 123:986–994

Iverson, R. (1997), *The physics of debris flows*, Rev. Geophys. 35:245–296

Matson, G. and Hogg, A. (2007), *Two-dimensional dam break flows of Herschel- Bulkley fluids: the approach to the arrested state*, J. Non-Newtonian Fluid Mech. 142 (2007) 79–94.

Parker, G., Fukushima, Y. and Pantin, H. (1986*), Self- accelerating turbidity currents,* J. Fluid Mech.171:145–181

Pritchard, D. (2005), *On fine sediment transport by a flood surge*, J. Fluid Mech 5343:239–248

Saint Venant, B (1871), *Théorie du mouvement non permanent des eaux, avec application aux crues des rivières et à l'introduction des marées dans leur lit*. C.R. Acad. Sci. sér. I 173:147–154– 237–240

Ritter, A (1892), *Die Fortpflanzung der Wasser-Wellen*, Zeitschrift des Vereines Deutscher Ingenieure 36(33):947–954